



MIGRATION OF U-SERIES RADIONUCLIDES AROUND THE BANGOMBE NATURAL FISSION REACTOR (GABON)

R. BROS¹, P. ROOS², N. YANASE¹, E. HOLM², H. ISOBE¹, T. SATO¹, Y. IIDA¹ and T. OHNUKI¹

1. JAERI, Environmental Geochemistry Laboratory, Tokai, Ibaraki, Japan
2. University of Lund, Department of Radiophysics, Lund, Sweden

1. INTRODUCTION

Investigations on the geochemistry of naturally occurring U-series radionuclides have been carried out on a natural nuclear reactor found in the Bangombé uranium deposit, about 30 km far from the main Oklo deposit. Due to its shallow location, this reactor has been weathered by the percolation of meteoric waters (Smellie and Winberg, 1993; Toulhoat et al., 1994; Bros et al., 1995; Louvat et al., 1995; Gurban, 1996). The Bangombé locality is unique in that the mobility of various actinides and fission products can be described in the reactor core and surrounding sediments (Bros et al., 1995), and also in the groundwaters which have been in contact with the reactor zone (Toulhoat et al., 1994). This allows the opportunity to evaluate and model the influence of groundwater chemistry and the different rock matrices on radionuclide mobilization/retardation processes. Evidence of such processes may be provided by the relative abundances of naturally occurring radionuclides, such as uranium, thorium, radium and lead. The main objective of the uranium-series disequilibrium studies in the Bangombé deposit is 1) to determine both the response of radionuclides to geochemical events affecting the reactor environment (lixiviation of the reactor core; dissolution-precipitation of secondary minerals; movements of redox fronts; transport of radionuclides; ...) and 2) to quantify the time-scale of geochemical events caused by groundwater flow which has been responsible for inducing disequilibrium. For example, $^{234}\text{U}/^{238}\text{U}$ and $^{230}\text{Th}/^{234}\text{U}$ disequilibria reflect geochemical processes which have occurred over the past 10^4 - 10^6 a. The ^{226}Ra - ^{230}Th pair can be used for processes occurring over periods varying from 1000 to 8000 years and the disequilibrium of the ^{210}Pb - ^{226}Ra pair reflects geochemical fractionation which took place during the last 150 years.

2. GEOLOGICAL SETTING

The uranium deposits of Mounana, Boyindzi, Oklo, Mikouloungou and of present concern Bangombé are located on the south-west border of the Franceville basin which is located in the south-eastern part of Gabon (fig. 1). The Francevillian is a very low grade metamorphic sedimentary, clastic and volcano-sedimentary series of lower proterozoic age (2100 Ma; Bros et al., 1992) which lies unconformably on an Archean crystalline basement. This series is composed of five units named FA at the base to FE at the top. The FA formation is composed of sandstones and conglomerates; the FB consists of black shales at the base and sandstones at the top of the unit; the FC, FD, FE units are mainly volcano-sedimentary with cherts and dolomite intercalations.

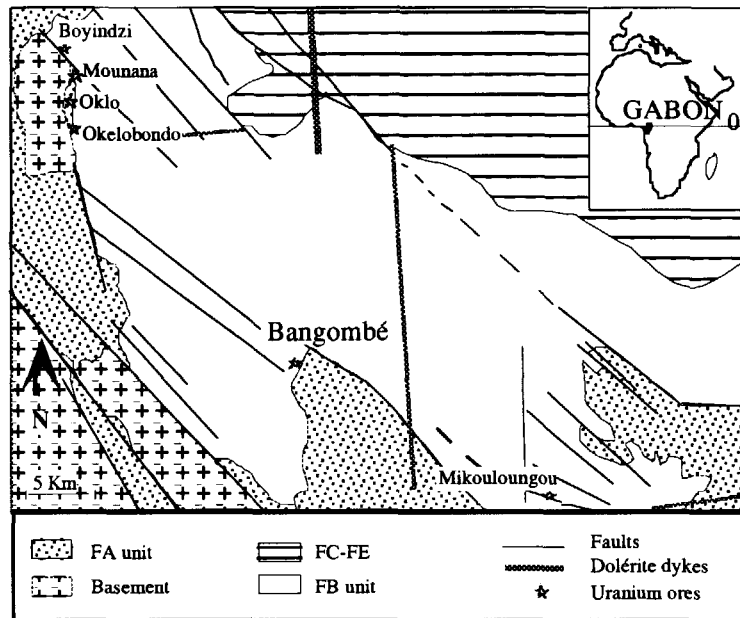


Figure 1 : Geological map of the Franceville basin (after Gauthier-Lafaye, 1986)

The basal FA formation contains all the uranium mineralizations discovered in the Franceville basin. The mineralization occurred very early during the oil diagenesis of the basin in oil traps formed during the first phase of structuration of the basin. Uranium has been transported by oxidizing fluids which altered U-enriched basal FA conglomerates and precipitated when these solutions met bitumens (Gauthier-Lafaye, 1986). The uranium mineralization has been dated to 2050 ± 30 Ma by the U-Pb method (Gancarz, 1978). During the concentration process, nuclear reactions could start in several specific areas when the critical mass of uranium has been reached (Naudet, 1991). The nuclear phenomenon caused desilicification of enclosing sandstones and new formation of clays around the core of the reactors (Gauthier-Lafaye, 1986). The reactor operation has been dated to 1970 Ma by Ruffenach (1979) using uranium, thorium and fissionogenic lanthanides. This age was confirmed by Holliger (1992) using the U-Pb method of dating. At present, 18 reactors have been discovered. The reactors 1 to 9 and "crochon" are located in the Oklo open quarry. The different studies performed on these reactors have been compiled by Naudet (1991) and Hagemann et al. (1980). Four reactors named 10, 13, 16 and OK84 were found in the south part of Oklo and in Okelobondo, the south extension of the deposit.

Bangombé is located 30 km far from Oklo, at the feet of the COMILOG manganese plateau (fig. 2, 4). This reactor is characterized by a very low depth (10-12 m) instead of 100-400 m for the Oklo and Okelobondo reactors. The deposit has a large area ($1,5 \text{ km}^2$) and it is characterized by a low uranium content (0.15 %) with local higher accumulations. As in Oklo and Okelobondo, the mineralized horizon is located in the upper part of the FA sandstones. The morphology of the ore is a large and slight anticlinal structure with a N-S to NE-SW fold axis plunging N to NE. The mineralization is located at the cartographic limit with the FB pelites, on the W limb of the upfold. Within this large structure, the Bangombé area defines an anticlinal structure with a NW-SE fold axis parallel to the Bangombé-Mambala fault and plunging 6° to the west. The mineralization of economic interest is associated to the top of this anticline.

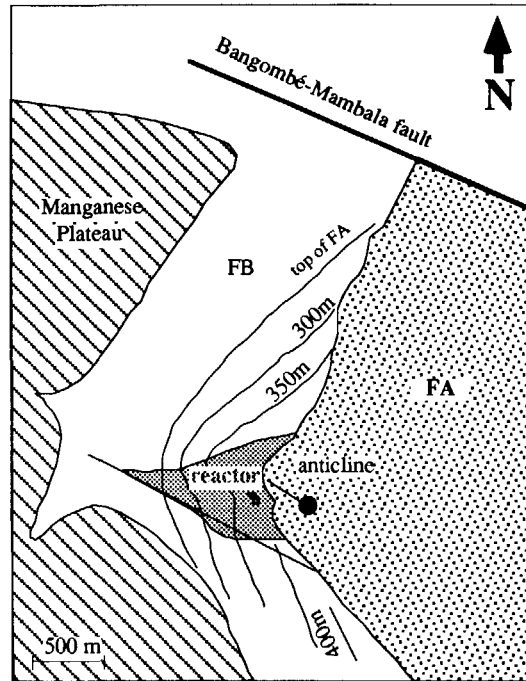


Figure 2 : Schematic geological map of the Bangombé area.

The Bangombé uranium deposit has been extensively investigated by drilling on a 20 x 20 m grid (fig. 3). The mineralized sandstones are 6 to 40 m deep within a unit denoted "a" and lenses of uranium are aligned with the axis of the anticline. The mineralization is limited to the wall by a thick unit of fine to pelitic sandstones, and to the top by FB pelites (fig. 4, 5). The uraniumiferous sandstones are generally middle to coarse grained generally devoided of sedimentary structures. Uranium is often linked to organic matter related to an hydraulic fracturing concordant to the bedding. The amount of uranium is estimated at 960 tonnes U (0,25 %) for the whole area (quarry + mine). The small quarry studied with a 20 x 20 m grid contain 180 tonnes U (0.2 %) including 40 tonnes of isotopically depleted U (1.2 %) in the reactor zone.

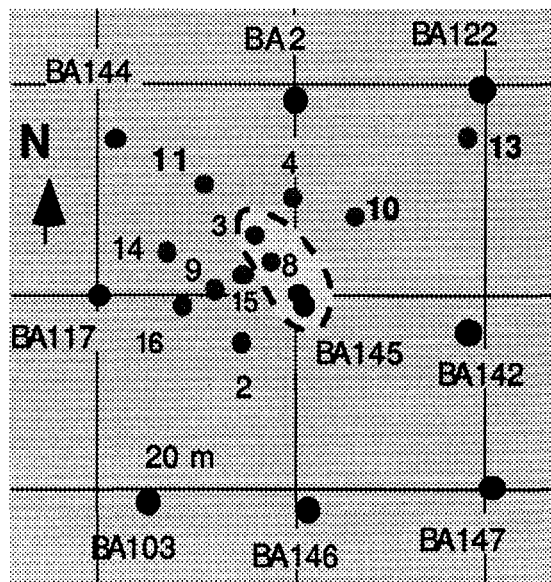


Figure 3 : Location of bore holes and possible shape of the reactor (dashes)

3. MATERIAL

The samples analyzed are drill-core sections collected during two field missions (Smellie and Winberg, 1991; Bros and Gauthier-Lafaye, 1996). As shown in figures 4 and 5, they have been collected at different depths along two vertical profiles (BAX 3; BAX 8) and at various lateral distances from the reactor zone (BAX15, BAX10, BAX13). A special attention was paid to the reactor core, the hydrothermal clays enclosing the reactor, the fracture filling material in mineralized sandstones, and the pelitic cover.

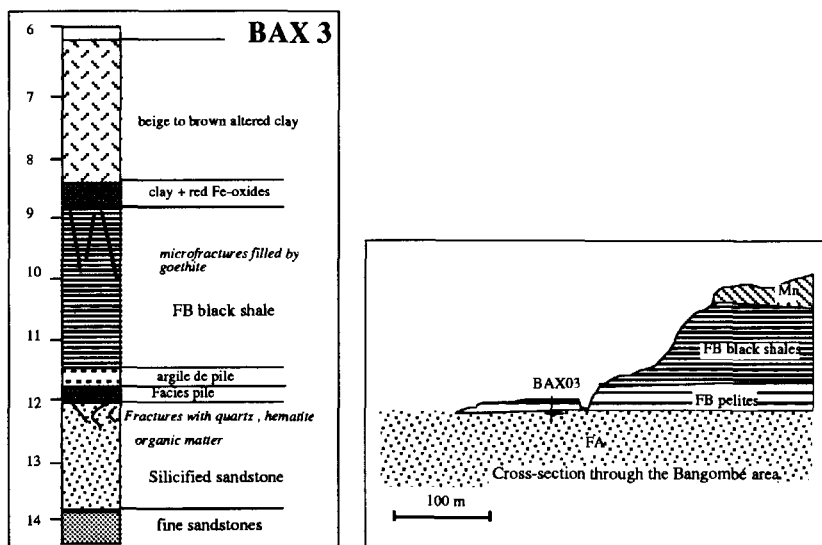


Figure 4: Schematic cross-section of the Bangombé deposit (after Smellie and Winberg, 1991) and the lithological log of drill-core BAX3

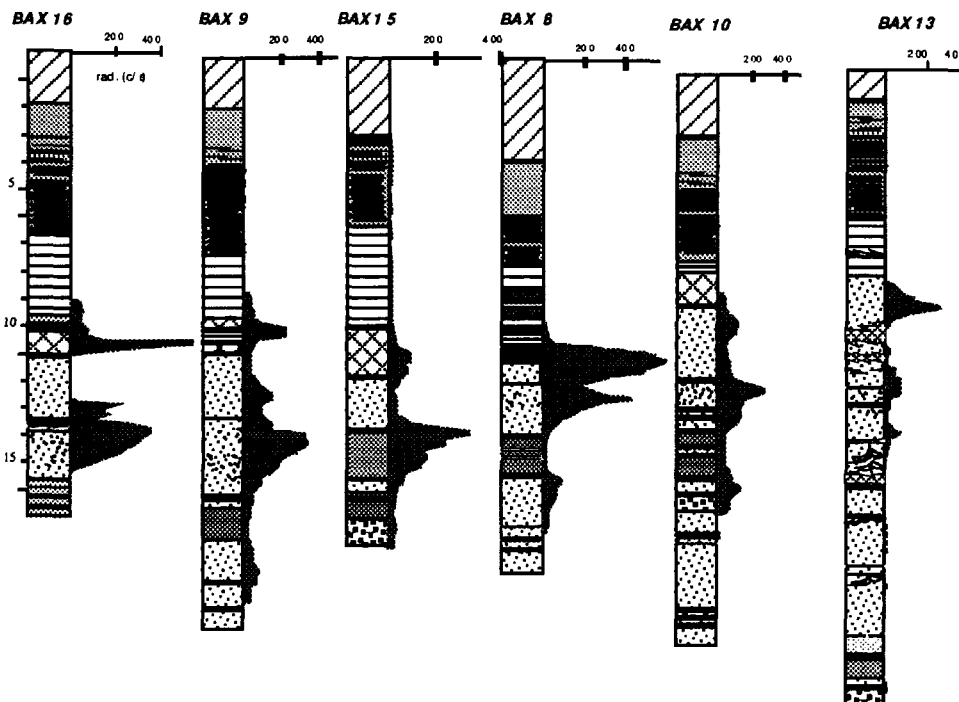


Figure 5 : Stratigraphic correlations at Bangomb é

4. EXPERIMENTAL

- Alpha spectrometry

For the radiochemistry of ^{238}U , ^{234}U and ^{230}Th isotopes, tracers (^{232}U , ^{229}Th) were added to the sample. The sample was dissolved in a HF-HNO₃-HCl mixture at 130°C, then loaded onto an anion-exchange column in chloride form (AG 1x4, 100-200 mesh). The fraction containing U was eluted with 8M HNO₃. Th was then eluted with 9M hydrochloric acid. U was extracted into tributyl phosphate (TBP) from the 8M HNO₃ eluant; then, U was recovered by back-extraction of the organic phase with distilled H₂O. Prior to extraction of U, the TBP was diluted with xylene to decrease the distribution coefficient of Th. Thorium and uranium in their respective solutions were electrodeposited onto a stainless steel disc from an ammonium sulphate electrolyte, the pH of which had been adjusted to fall within the range of 2.1 to 2.4 using concentrated ammonia solution. A current of 1 A was applied for one hour, after which the electrolyte was quenched with ammonia and the disc was removed. The α -spectrometry of the electroplated discs was carried out using silicon ion-implanted detectors, with sensitive areas of 300 mm². The resolution was 30-40 keV throughout the region of interest from 4.15 MeV to 5.31 MeV. Recoveries for thorium and uranium averaged 92% and 65%, respectively.

- Gamma spectrometry

4 g of powdered samples were placed into a planar plastic vessel whose inner diameter is 60 mm (Yanase and Sekine, 1995). The thickness of the sample was adjusted to less than 1.4 mm to minimize the self-absorption effect. Measurements were done using an ORTEC LO-AX germanium detector with 0.5 mm-thick beryllium window connected to a SEIKO EG&G 7800 MCA (multichannel analyzer). The gamma rays used were ^{231}Pa (27.4 keV), ^{210}Pb (46.5 keV), ^{234}Th (63.0 keV) for ^{238}U determination, ^{230}Th (67.7 keV), ^{235}U (163 keV), ^{226}Ra (186 keV). All these peaks are single ones, except for ^{226}Ra whose contribution of ^{235}U to the 186 keV was subtracted, using the counts at the 63 keV peak.

- Selective extraction procedure

About 4 g of powdered material was shaken at room temperature for 4 hours with 40 ml of 1M sodium acetate adjusted to pH 5.0 by acetic acid. The extraction with Na acetate solution is thought to remove the adsorbed/exchangeable trace metals and those associated with carbonate phases (Morgan, 1935; Payne, 1985). At the end of the extraction, the suspended solution was separated by a combination of centrifugation and filtration using a 0.1 μm Millipore filter (Yanase et al., 1991).

5. RESULTS AND DISCUSSION:

5.a. Spatial distribution of ^{238}U , ^{234}U and ^{230}Th radionuclides

The radiochemical data obtained by α -spectrometry are presented in Tables 1 and 2 which include the activity of ^{238}U (mBq/g) and the $^{230}\text{Th}/^{234}\text{U}$ and $^{234}\text{U}/^{238}\text{U}$ activity ratios.

Core	Depth (m)	Facies	^{238}U mBq/g	$^{234}\text{U}/^{238}\text{U}$ activity ratio	$^{230}\text{Th}/^{234}\text{U}$ activity ratio
BAX 3	7.85	beige clay	153.7	1.08 (0.01)	0.98 (0.02)
BAX 3	8.54	red clay	949.2	1.08 (0.02)	0.89 (0.02)
BAX 3	9.40	red clay	1654.3	1.01 (0.02)	0.87 (0.03)
BAX 3	10.25	black shale	1093.1	1.13 (0.02)	0.96 (0.04)
BAX 3	10.83	black shale	510.0	1.08 (0.01)	0.98 (0.03)
BAX 3	11.53	black shale	12273	0.90 (0.02)	0.95 (0.03)
BAX 3	11.70	hydrothermal clay	28084	1.02 (0.02)	0.98 (0.03)
BAX 3	11.75	hydrothermal clay	24241	1.04 (0.01)	1.59 (0.03)
BAX 3	11.80	reactor core	6145689	1.00 (0.02)	1.05 (0.02)
BAX 3	12.00	hydrothermal clay	33599	1.00 (0.02)	1.27 (0.04)
BAX 3	12.92	fracture	19044	0.95 (0.01)	1.12 (0.02)
BAX 3	13.17	fracture	17666	0.98 (0.02)	1.10 (0.03)
BAX 3	13.81	fracture	16275	0.99 (0.02)	1.05 (0.02)
BAX 3	14.06	fracture	1754	1.00 (0.03)	1.00 (0.03)
BAX 10	12.30	fracture	41446	0.96 (0.03)	1.03 (0.02)
BAX 13	10.90	oxidized sandstone	2930	0.92 (0.03)	1.07 (0.03)
BAX 13	15.25	oxidized sandstone	4042	1.02 (0.02)	1.16 (0.04)
BAX 13	18.60	fracture clay	4048	0.59 (0.02)	1.04 (0.02)
BAX 13	20.45	oxidized sandstone	56.1	1.21 (0.02)	0.71 (0.03)
BAX 15	11.55	Fe-oxide fracture	16063	1.07 (0.03)	1.00 (0.03)
BAX 15	13.05	Fe-oxide fracture	13448	1.06 (0.02)	0.76 (0.04)

Table 1: Activity of ^{238}U (mBq/g) and $^{234}\text{U}/^{238}\text{U}$, $^{230}\text{Th}/^{234}\text{U}$ activity ratios of drill-cores BAX 3, BAX 10, BAX 13, BAX 15.

Based on a Thiel diagram (Thiel et al., 1983), figure 6 shows how the fractionating processes of leaching, recoil mobilization and precipitation can affect the relative abundances of ^{238}U and its successive daughters ^{234}U and ^{230}Th . The center of the diagram marks the point where both activity ratios are at unity and the U-series radionuclides are in secular radioactive equilibrium. In this plot there are two contrasting halves separated by a diagonal line marking where ^{230}Th is in equilibrium with ^{234}U . To the lower right part of the diagram, chemical leaching has mobilized ^{234}U leaving the ^{230}Th daughter in relative excess. To the upper left, accumulation/precipitation of the previously mobilized U produce an excess of ^{234}U relative to ^{230}Th . The second major dividing line in the plot is the horizontal line defined by a $^{234}\text{U}/^{238}\text{U}$ activity ratio of 1. Below this line there is a ^{234}U deficiency relative to ^{238}U , the result of ^{234}U recoil mobilization. Above this line there is an excess of ^{234}U , the

consequence of ^{234}U deposition. Significant disequilibria for $^{234}\text{U}/^{238}\text{U}$ and $^{230}\text{Th}/^{234}\text{U}$ parent-daughter pairs are characteristic for most of the samples, indicating that the Bangombé geochemical system has not been a closed system, at least during the last 1 Ma. Since ^{230}Th is comparatively immobile and characterized by a extremely low solubility in natural waters (Kaufman, 1969), the disequilibria are mainly due to preferential mobilization of uranium isotopes. The data define a rough horizontal trend and, for most of the samples, the $^{230}\text{Th}/^{234}\text{U}$ ratio deviates from unity indicating that the rate of uranium mobilization is too rapid or very recent to allow ^{230}Th to reequilibrate with its precursor ^{234}U (requiring at least 350 Ka) while leaving, in some cases, ^{234}U in disequilibrium with its parent ^{238}U (requiring 1.5 Ma to restore equilibrium). A striking exception is the clay infilling material from a vertical, opened fracture (BAX13) which has a low $^{234}\text{U}/^{238}\text{U}$ ratio (0.59 ± 0.02) and a $^{230}\text{Th}/^{234}\text{U}$ activity ratio close to 1. This may indicate a preferential leaching of ^{234}U resulting from alpha-recoil mechanism (Griffault et al., 1993) which is either extremely slow or sufficiently old ($350 \text{ Ka} < T < 1.5 \text{ Ma}$) to allow ingrowth of ^{230}Th to reach a state of equilibrium while leaving ^{234}U in strong deficiency relative to ^{238}U .

Core	Depth (m)	Facies	^{238}U mBq/g	$^{234}\text{U}/^{238}\text{U}$ activity ratio	$^{230}\text{Th}/^{234}\text{U}$ activity ratio
BAX 8	2.70	soil	54.3	1.05 (0.01)	0.95 (0.03)
BAX 8	3.00	soil	130.5	1.07 (0.02)	0.90 (0.03)
BAX 8	3.45	soil	45.5	1.24 (0.01)	0.80 (0.04)
BAX 8	3.97	soil	70.8	1.18 (0.01)	0.85 (0.03)
BAX 8	4.85	ocher clay	32.2	1.00 (0.02)	0.79 (0.02)
BAX 8	5.45	ocher clay	33.3	0.98 (0.02)	0.58 (0.02)
BAX 8	5.70	pink clay	42.7	1.02 (0.01)	0.78 (0.03)
BAX 8	6.10	ocher clay	53.1	1.02 (0.01)	0.75 (0.03)
BAX 8	6.45	white clay	102.8	0.99 (0.01)	0.94 (0.03)
BAX 8	6.85	white clay	267.2	0.97 (0.02)	0.94 (0.04)
BAX 8	7.20	ocher clay	627.1	0.98 (0.01)	0.87 (0.05)
BAX 8	8.50	black shale	125.9	1.07 (0.01)	0.93 (0.04)
BAX 8	9.14	Fe crust	3077	0.98 (0.01)	0.80 (0.02)
BAX 8	10.30	Fe crust	4367	0.90 (0.02)	0.66 (0.03)
BAX 8	10.52	Fe crust	2960	1.08 (0.02)	1.09 (0.04)
BAX 8	10.90	hydrothermal clay	22276	1.11 (0.01)	0.93 (0.03)
BAX 8	10.90	reactor core	6703290	0.98 (0.02)	0.99 (0.04)
BAX 8	12.10	Fe-oxide fracture	11351	1.01 (0.01)	1.87 (0.05)

Table 2 : Activity of ^{238}U (mBq/g), $^{234}\text{U}/^{238}\text{U}$ and $^{230}\text{Th}/^{234}\text{U}$ activity ratios of samples from drill-core BAX 8.

- one reactor core sample (BAX 8; 10.90 m) shows secular equilibrium for the $^{234}\text{U}/^{238}\text{U}$ and $^{230}\text{Th}/^{234}\text{U}$ activity ratios which indicates the stability of irradiated uraninite during the last 1.5 Ma. Another core sample (BAX 3; 11.80 m) has a $^{234}\text{U}/^{238}\text{U}$ activity ratio of 1 and a $^{230}\text{Th}/^{234}\text{U}$ activity ratio slightly greater than unity (1.05 ± 0.02) which suggest a low and recent ($< 350 \text{ Ka}$) leaching

of ^{234}U from the core.

- the hydrothermal clays (BAX 3; 11.75 m and 12.00 m) and fracture fillings beneath the reactor zone (BAX 3, 12.00 m; BAX 8; 12.10 m) are characterized by high $^{230}\text{Th}/^{234}\text{U}$ activity ratio (up to 1.87) and $^{234}\text{U}/^{238}\text{U}$ activity ratio at equilibrium or near equilibrium. Therefore, mobilization of uranium took place recently (< 350 Ka) caused by circulation of pore waters of meteoric origin. A possible explanation is the existence of local oxidizing conditions at the immediate vicinity of the reactor core related to 1) high groundwater flow at the sandstones/shales interface which indicates enhanced hydraulic conductivity, and 2) the possible radiolysis of water near the high-grade uranium ore leading to oxidation of U(IV) to U(VI) state and its subsequent leaching and removal. The former mechanism is the more probable since a rapid groundwater flow is contradictory with sufficient build-up of oxidants (e.g. O_2 , H_2O_2) induced by water radiolysis, to mobilize uranium.

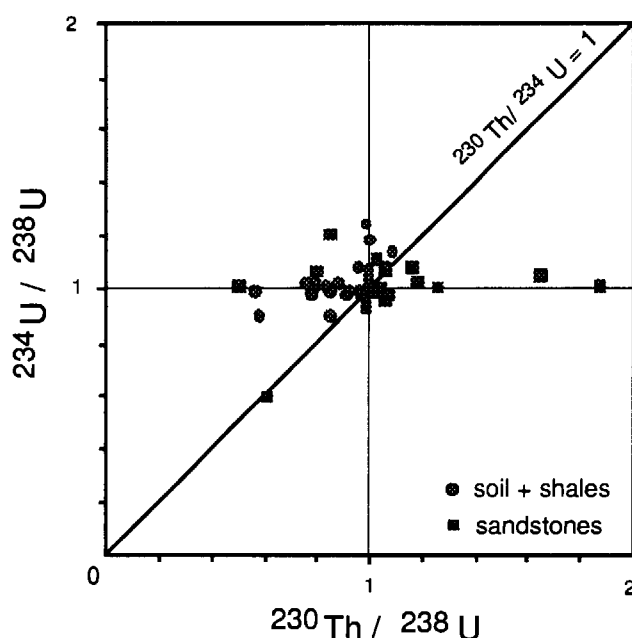


Figure 6 : $^{230}\text{Th}/^{238}\text{U}$ and $^{234}\text{U}/^{238}\text{U}$ activity ratios of samples from Bangomb é plotted on a Thiel diagram (Thiel et al., 1983)

- porous and oxidized sandstones from BAX 13 display various isotopic signatures. The sample located at 10.90 m has a $^{234}\text{U}/^{238}\text{U}$ activity ratio slightly lower than unity (0.92 ± 0.03) and a $^{230}\text{Th}/^{238}\text{U}$ activity ratio of unity. This indicates a rapid or recent preferential mobilization of ^{234}U induced by alpha-recoil effect. The sample collected at 15.25 m shows a $^{234}\text{U}/^{238}\text{U}$ activity ratio of unity and a $^{230}\text{Th}/^{238}\text{U}$ activity ratio greater than unity (1.16 ± 0.04) which indicate a rapid or recent chemical leaching of ^{238}U without any fractionation of uranium isotopes. The deepest sandstone (20,45 m) is in excess of ^{234}U relative to ^{238}U ($^{234}\text{U}/^{238}\text{U} = 1.21 \pm 0.02$) and the $^{230}\text{Th}/^{238}\text{U}$ activity ratio is lower than unity (0.86 ± 0.03). This suggests a preferential accumulation of ^{234}U (because of recoil processes) in this sample which is comparatively less oxidized and contains remnants of old, detrital organic matter, therefore decreasing the redox potential and enhancing the fixation of mobile uranium having a relatively high $^{234}\text{U}/^{238}\text{U}$ activity ratio.

- in the shale cover and the uppermost shallow soil, all the samples strikingly fall on the upper left part of the diagram where ^{234}U is in excess of ^{230}Th (fig. 6). Therefore, these levels correspond to

zones of accumulation where recent (<350 Ka) precipitation of previously mobilized uranium has produced an excess of ^{234}U relative to its daughter ^{230}Th . Soil samples have $^{234}\text{U}/^{238}\text{U}$ activity ratio greater than unity and $^{230}\text{Th}/^{238}\text{U}$ activity ratio at or near unity, resulting from the recent fixation of uranium enriched in ^{234}U by alpha-recoil mechanisms. The second major group corresponds to oxidized pelites having $^{234}\text{U}/^{238}\text{U}$ activity ratio at unity and $^{230}\text{Th}/^{238}\text{U}$ activity ratio significantly lower than unity. This disequilibrium pattern results from the rapid accumulation of ^{238}U without fractionation of the $^{234}\text{U}/^{238}\text{U}$ activity ratio. These aspects are discussed in further details in the next chapters.

BAX 3 profile :

Considering the $^{234}\text{U}/^{238}\text{U}$ and $^{230}\text{Th}/^{234}\text{U}$ activity ratios, 3 zones can be identified (fig. 7) :

- a) A zone (11.75 to 14.06 m) which includes the reactor core, hydrothermal clays and underlying open fractures within the mineralized sandstones. In this zone, the highest $^{230}\text{Th}/^{234}\text{U}$ activity ratios have been measured, i.e. 1.27 and 1.59 in the hydrothermal clays located at 12 m and 11.75 m, respectively. Since the $^{234}\text{U}/^{238}\text{U}$ activity ratio is close to unity, this implies a recent and rapid removal of uranium at the immediate vicinity of the reactor. The $^{230}\text{Th}/^{234}\text{U}$ activity ratio decreases progressively with increasing depth until unity is achieved at 14.06 m. This suggests the existence of a gradient of uranium removal which is greatest at the immediate vicinity of the reactor and tends to decrease in low-grade mineralized areas.

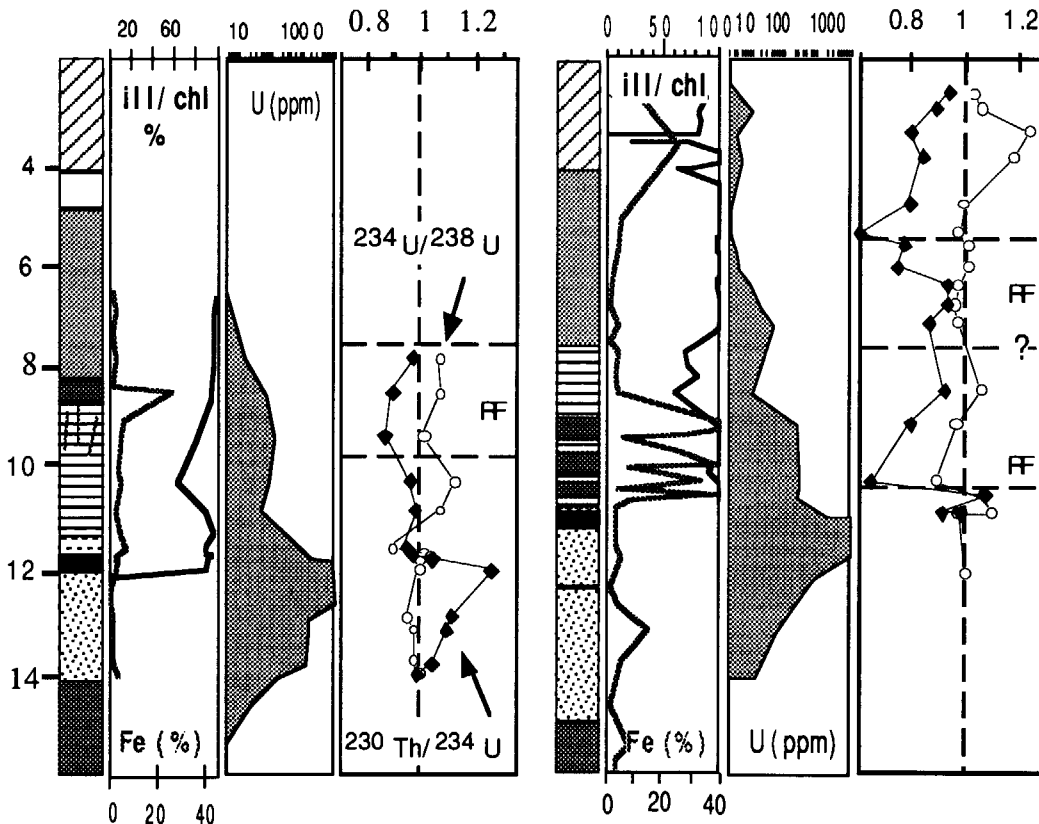


Figure 7 : $^{234}\text{U}/^{238}\text{U}$ and $^{230}\text{Th}/^{234}\text{U}$ activity ratios along BAX 3 and BAX 8 drill-cores. The Fe content and illite/chlorite ratio of BAX 3 and BAX 8 are from Bros et al. (1995), Salah and Gauthier-Lafaye (1997, 1998).

- b) A black shale layer (10.25 to 11.53 m) where the $^{234}\text{U}/^{238}\text{U}$ activity ratio increases with decreasing depth. The $^{234}\text{U}/^{238}\text{U}$ activity ratio is lower than unity in the basal black shale (0.90 ± 0.02) and reaches a maximum value (1.13 ± 0.02) at 10.25 m which also corresponds to the highest content of chlorite. This suggests upward, preferential migration of ^{234}U (related to recoil-mobilization processes) and fixation by shales under reducing conditions, as indicated by the high chlorite content. This process is in accordance with upward migration of fissionogenic REEs reported in previous studies (Bros et al., 1995). The $^{230}\text{Th}/^{234}\text{U}$ activity ratio is unity at 10.83 m and 10.25 m which indicates that the accumulation of ^{234}U is slow, or that the deposition is old ($> 350\ 000$ ka), i.e. in both cases subsequent ingrowth of ^{230}Th has achieved a state of transient equilibrium.
- c) A level of oxidized pelites (7.85 to 9.40 m) having $^{234}\text{U}/^{238}\text{U}$ activity ratios slightly greater than unity. A decrease of the $^{230}\text{Th}/^{234}\text{U}$ activity ratio with increasing depth is observed, which reaches a lowest value of 0.87 at 9.40 m. This is accompanied by a progressive increase of the U content (3.8 to 135.6 ppm) and chlorite content. This indicates the downward penetration of a redox front which has caused the disappearance of organic matter, the dissolution of inherited minerals (mostly chlorite), and the gradual removal/precipitation of uranium towards the bottom. This redox front did not affect the reactor. The main accumulation of uranium is located at 9.40 m and petrographically marked by the occurrence of small sub-vertical veins filled by goethite, which progressively replaces the shale clayey matrix towards the bottom.

The rate of frontal movement R can be deduced with a certain level of confidence, considering the distance d between the highest $^{230}\text{Th}/^{234}\text{U}$ activity ratio of unity and the minima :

$$R = d / T_{230} \quad T_{230} = 75\ 200 \ln 2 = 108.5 \text{ Ka} \quad (\text{Osmond et al., 1983})$$

The estimated rate of downward redox front movement is 1.5 m / 100 000 years (1.5 cm Ka^{-1}), assuming a distance of 1.6 m.

BAX 8 profile :

- a) In the soil which forms the uppermost part of BAX 8 (2.70 m to 3.97 m), the $^{230}\text{Th}/^{238}\text{U}$ activity ratio is at or near unity. The $^{234}\text{U}/^{238}\text{U}$ activity ratio is greater than unity and the activity of ^{238}U (54.3 to 130.5 mBq/g) is higher than in underlying weathered pelites. These excesses are ascribed to the presence of humic substances produced by decomposition of plants and roots at this level. Organic substances having high complexation capacities (Zhang et al., 1996) may have fixed recently uranium enriched in ^{234}U supplied by surface waters circulating through the soil. The $^{234}\text{U}/^{238}\text{U}$ activity ratio increases with increasing depth (up to 1.24). This indicates the increase of the reducing capacity of the soil with increasing depth and the loss of the oxidizing capacity of surface waters.

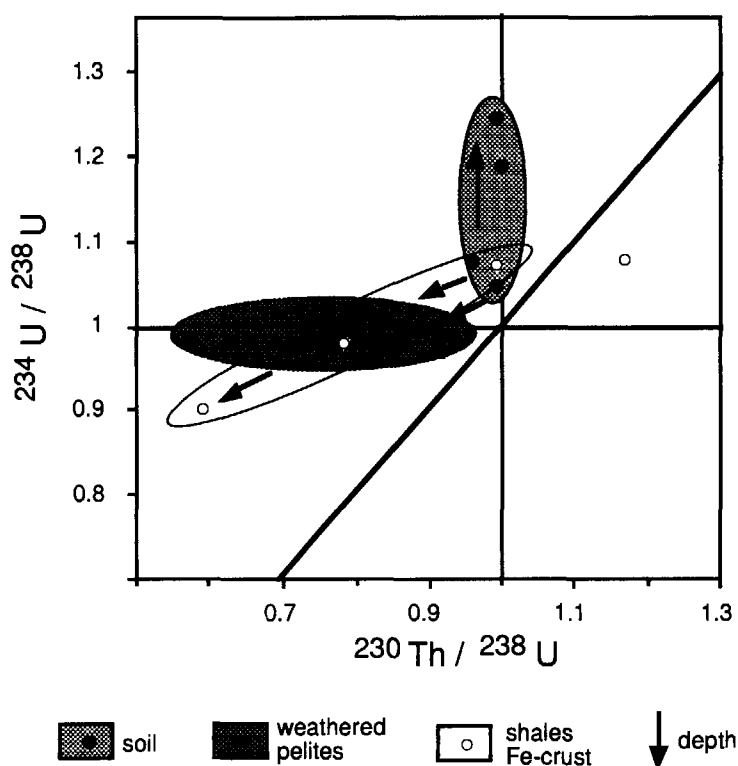


Figure 8 : $^{230}\text{Th}/^{238}\text{U}$ and $^{234}\text{U}/^{238}\text{U}$ activity ratios of BAX 8 samples

- b) In weathered pelites (4.85 m to 7.20 m), illite is the main component with minor feldspar, goethite and hematite, and chlorite is absent (Salah and Gauthier-Lafaye, 1997). The $^{234}\text{U}/^{238}\text{U}$ activity ratio is at or near unity and the U content records low values (2.6 to 4.3 ppm) between 4.85 m and 6.10 m. This is contradictory with low $^{230}\text{Th}/^{234}\text{U}$ activity ratio (down to 0.58 at 5.45 m) which indicates a rapid accumulation of uranium without fractionation of the $^{234}\text{U}/^{238}\text{U}$ activity ratio. Therefore, two stages are considered: a old oxidative leaching when dissolution of chlorite and intense removal of uranium took place, followed by a recent (<350 000 Ka) fixation of low quantities of U onto weathered pelites.
- c) In deeper weathered pelites (6.45 m to 7.20 m), the $^{234}\text{U}/^{238}\text{U}$ activity ratio is at or near unity. The activity of ^{238}U increases with increasing depth (103 to 627 mBq/g) and the $^{230}\text{Th}/^{234}\text{U}$ activity ratio decreases from 0.94 to 0.87. The lower $^{230}\text{Th}/^{234}\text{U}$ activity ratio at 7.20 m is related to a relatively high amount of goethite and the absence of chlorite (Salah and Gauthier-Lafaye, 1997). Therefore, this zone may correspond to the upflow of a downwardly penetrating oxidizing front which caused the dissolution of chlorite, the newformation of goethite and the remobilization/reprecipitation of uranium towards the bottom, the same process as described in BAX 3 (see previous chapter). The main accumulation of uranium is thought to have occurred between 7.20 and 8.50 m, although the lack of data so far do not allow to precise its location.
- d) In a level of reduced black shales (8.50 m) and Fe crusts (9.14 m; 10.30 m; 10.52 m) enriched in goethite and hematite, the activity of ^{238}U reaches high values in deep samples, up to 4367 mBq/g. From 10.30 m to 8.50 m, the $^{234}\text{U}/^{238}\text{U}$ activity ratio increases from 0.90 to 1.07, and the $^{230}\text{Th}/^{234}\text{U}$ activity ratio increases from 0.66 to 0.93. In a Thiel diagram (fig. 8), the $^{234}\text{U}/^{238}\text{U}$

and $^{230}\text{Th}/^{238}\text{U}$ activity ratios display a nearly linear relationship and both activity ratios increase with decreasing depth. This disequilibrium pattern suggests 1) an upward preferential mobilization of ^{234}U (caused by recoil mechanisms) towards the top of the shales, and 2) a downward removal/precipitation of uranium related to a redox front which is marked by important accumulations of Fe (III) minerals (goethite, hematite) and high U concentrations. This front affected the deepest shales in BAX 8, which is not the case in BAX 3. The existence of two oxidized zones separated by a reduced shale layer in BAX 8 can be explained by the fracturation of shales, a possible pathway for oxidizing waters coming from the surface.

- e) The Fe-oxide crust located at 10.52 m, immediately above the reactor display different characteristics. It falls in the "forbidden zone", corresponding to the situation in which ^{234}U is at the same time in excess of ^{238}U and deficient relative to ^{230}Th (Osmond et al., 1983). This can be explained by the influence of lateral circulations of groundwaters at the sandstones/shales interface and by a complex multi-stage history (i.e. not steady state system) with sudden changes in flow regime at this level.

Core; depth (m)	^{234}Th 24.1 d	^{230}Th 75 200 y	^{226}Ra 1602 y	^{214}Pb 26.8 m	^{214}Bi 19.7 m	^{210}Pb 22 y
BAX3; 6.52	0.048 (7)	-	-	0.045 (4)	0.046 (3)	0.049 (3)
BAX3; 6.90	0.068 (5)	-	0.057 (9)	ND	0.067 (2)	0.617 (7)
BAX3; 7.85	0.16 (2)	-	0.12 (1)	0.13 (1)	0.13 (2)	0.19 (1)
BAX3; 8.54	0.78 (1)	0.83 (5)	0.65 (2)	ND	0.70 (1)	0.73 (1)
BAX3; 9.40	1.46 (2)	1.11 (9)	2.40 (4)	ND	2.19 (1)	2.66 (3)
BAX3; 10.25	1.15 (7)	2.21 (9)	-	1.40 (5)	1.35 (5)	1.92 (7)
BAX3; 10.83	0.55 (4)	0.73 (8)	0.82 (7)	0.59 (3)	0.56 (2)	0.92 (4)
BAX3; 11.70	35 (3)	55 (6)	41 (2)	33 (2)	32 (2)	45 (2)
BAX3; 11.75	25 (2)	37 (6)	137 (5)	106 (5)	107 (4)	156 (7)
BAX3 11.75Mor*	7.76 (1)	-	64.77 (1)	ND	4.46 (2)	45.39 (1)
BAX3; 11.80 FP	7220 (29)	6390 (96)	7920 (40)	ND	8710 (9)	4740 (19)
BAX3; 12.15	1290 (55)	1753 (79)	1015 (50)	1108 (38)	1182 (48)	614 (22)
BAX3; 13.17	18.1 (9)	29 (2)	19 (1)	20 (1)	19 (1)	30 (2)
BAX3; 14.06	1.8 (2)	5.3 (9)	34 (1)	26.3 (9)	27.5 (8)	38.2 (9)
BAX8; 10.30	4.48 (3)	2.9 (1)	3.14 (5)	ND	2.98 (1)	3.22 (2)
BAX8; 10.52	2.93 (4)	3.5 (2)	6.05 (7)	ND	4.85 (2)	6.21 (5)
BAX8; 10.90 AP	20.3 (2)	24.8 (9)	107 (1)	ND	87.6 (2)	209 (1)
BAX8; 10.90 FP	7100 (21)	6430 (83)	7280 (36)	ND	7810 (8)	4030 (16)
BAX8; 12.10	13.7 (7)	30.5 (4)	33.3 (9)	ND	23.2 (1)	36.9 (1)
BAX15; 13.05	13.8 (3)	11.3 (4)	9.4 (2)	ND	8.2 (1)	9.9 (1)

Table 3 : Activity of ^{234}Th , ^{230}Th , ^{226}Ra , ^{214}Pb , ^{214}Bi , ^{210}Pb expressed in Bq/g and determined by γ spectrometry. AP = argile de pile (hydrothermal clay); FP = faciès pile (reactor core); Mor = Morgan's solution (Na acetate); * = activity calculated for 1 g of leached powder; ND = not determined.

5.b. ^{226}Ra - ^{230}Th disequilibria

Radiochemical data obtained by γ -spectrometry are shown in Table 3 which include the activity of ^{234}Th , ^{230}Th , ^{226}Ra , ^{214}Pb , ^{214}Bi and ^{210}Pb . ^{226}Ra ($t_{1/2} = 1602$ years) is commonly found in excess relative to its immediate precursor ^{230}Th in natural groundwaters due to the higher solubility of Ra. The activity of radium varies from 0.1 Bq l^{-1} in diluted surface waters to 20 Bq l^{-1} in brines (Gascoyne, 1989). This generally leads to a depletion of ^{226}Ra relative to ^{230}Th in rocks that have been altered recently. At Bangombé, several zones are identified regarding the variations of the $^{226}\text{Ra}/^{230}\text{Th}$ activity ratio :

- ◆ In the reactor core, ^{226}Ra is in slight excess relative to its precursor ^{230}Th . The $^{226}\text{Ra}/^{230}\text{Th}$ activity ratio is 1.24 in sample BAX3 / 11.80 m and 1.13 for sample BAX8 / 10.90 m. This indicates a recent (< 8000 years) uptake of Ra vehiculated by groundwaters.
- ◆ In hydrothermal clays located at the immediate vicinity of the high-grade U-ore, ^{226}Ra is in significant excess relative to ^{230}Th . The $^{226}\text{Ra}/^{230}\text{Th}$ activity ratio is 3.7 in sample BAX3 / 11.75 m and 4.3 in sample BAX8 / 10.90 m. This also indicates a recent accumulation of Ra from groundwaters at this depth. The activity of ^{226}Ra in the Morgan solution (sample BAX3 / 11.75 m) is 65 Bq per gram of leached sample, representing half of the total activity of the sample. Since there is no carbonate in the sample, most of this excess ^{226}Ra is thought to be adsorbed onto clay minerals.

5.c. Short-lived ^{214}Pb , ^{214}Bi and ^{210}Pb

- ◆ In the reactor core, ^{210}Pb ($t_{1/2} = 22 \text{ y}$) is significantly depleted relative to ^{226}Ra and its short-lived precursor ^{214}Bi ($t_{1/2} = 19.7 \text{ m}$). The $^{210}\text{Pb}/^{226}\text{Ra}$ activity ratio is 0.6 in sample BAX3/11.80 m and 0.55 in sample BAX8/10.90 m. This suggests a recent (< 100 years) loss of Pb from uraninite and subsequent leaching by groundwaters.
- ◆ In hydrothermal clays, ^{210}Pb is in excess relative to ^{226}Ra ; the $^{210}\text{Pb}/^{226}\text{Ra}$ activity ratio is 1.14 in sample BAX3/11.75 m and 1.95 in sample BAX8/10.90 m. Therefore, as described in the previous section, Pb which has been removed from uraninite appears to have been accumulated recently ($< 100 \text{ y.}$) onto clays located at the immediate vicinity of the reactor. The low $^{214}\text{Bi}/^{226}\text{Ra}$ activity ratio of these samples (0.78 in BAX3/11.75 m; 0.82 in BAX8/10.90 m) is ascribed to a recent loss of intermediate ^{222}Rn radionuclide ($t_{1/2} = 3.8 \text{ d}$) by gaseous diffusion.
- ◆ In reducing black shales and oxidized/shallow pelites, like for hydrothermal clays, ^{210}Pb is also in significant excess relative to ^{226}Ra . The $^{210}\text{Pb}/^{226}\text{Ra}$ activity ratio ranges from 1.02 to 1.58 and reaches a high value of 10.8 in sample BAX3/6.90 m which corresponds to a zone where Pb has accumulated during the last century.

6. Conclusion - A conceptual model for the spatio/temporal evolution of Bangombé

Schematically represented on Figure 9 is a proposed model for the evolution of the Bangombé system. The strongest disequilibria are found in the hydrothermal clay halo and along the uppermost sandstone fractures located at the immediate vicinity of the reactor core (BAX 3, BAX 8). The high rate of uranium mobilization at this depth may be attributed to lateral circulation of oxidizing groundwaters at the sandstones/shales interface which is thought to be a zone of high hydraulic conductivity. Less likely is the possible radiolysis of water at the contact with the reactor zone and the high-grade mineralization leading to the oxidation of U (IV) to U (VI) and its subsequent removal and transport towards the far-field.

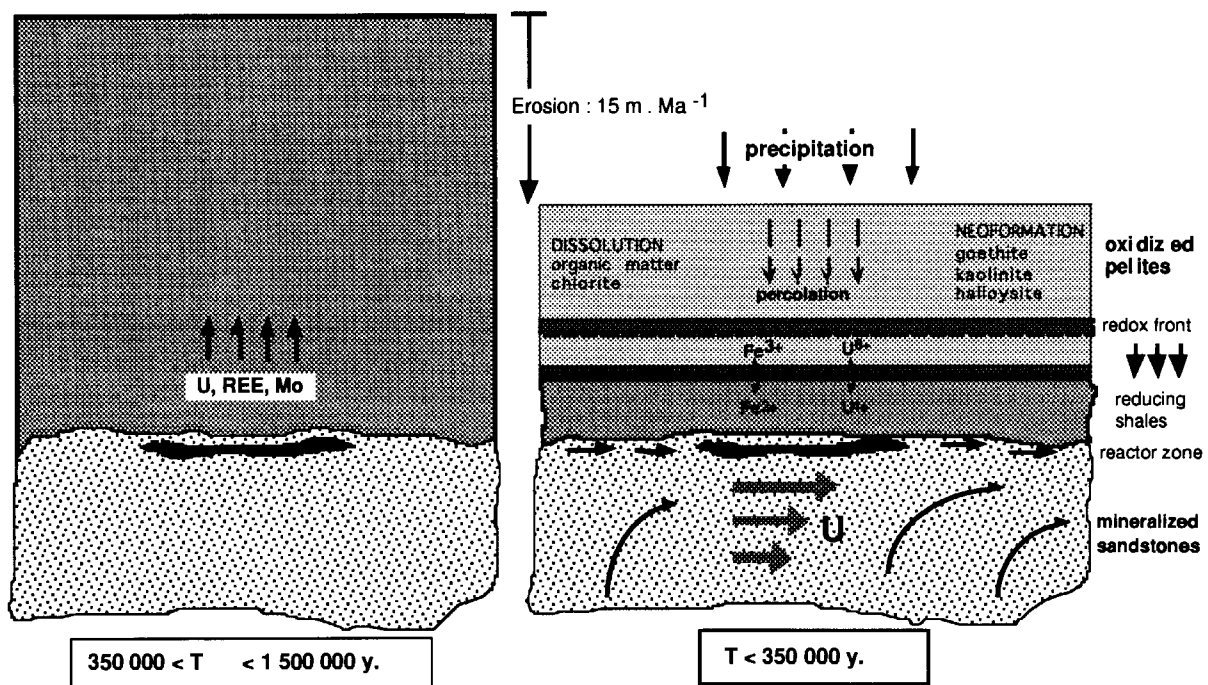


Figure 9 : Hypothetic evolution of the Bangombé system; lithological units, mineralogical transformations and mass-transfers incurred during supergene alteration and along possible groundwater pathways

Above the reactor zone, upward migrations and fixation of uranium took place recently, although the mechanism of transport (advective transport or simple diffusion) is not clearly understood so far. This process is related to upward migrations of ²³⁵U-depleted uranium and fission products released from the reactor core (rare-earth elements, molybdenum) which has been previously reported (Bros et al., 1995). The upper part of the shales shows oxidation effects related to the percolation of oxygenated waters from the surface. This has produced downward migrating redox fronts which dissolve inherited mineral phases, mostly Fe(II)-bearing chlorite, producing secondary alteration phases such as goethite, kaolinite and halloysite. Coevally, uranium has been dissolved, transported and reprecipitated near the bottom of the shales. At the redox interface, Fe (II) is oxidized to Fe (III) and precipitates as goethite, while U(IV) is oxidized to U(VI). The U/Fe coupling at the

oxidizing/reducing interface resulted in the coprecipitation and/or the scavenging of U(VI) by sorption onto the surface of precipitated Fe (III) goethite (Bruno et al., 1995). Although difficult to estimate with a high level of accuracy, the chronology and time-scale of migration events can be deduced. Two possible models of evolution for groundwater flow and the related transport of uranium are suggested: 1) a competitive oscillation of upward and downward effects which can be explained by fluctuations of the water table. The accumulation of uranium towards the top is slow and allows ingrowth of ^{230}Th to reach a state of radioactive equilibrium. The accumulation of uranium towards the bottom is comparatively far more rapid as indicated by strong disequilibria of the $^{230}\text{Th}/^{234}\text{U}$ activity ratio; 2) more probable, a discontinuous evolution in which upward and downward migrations of uranium took place at two different stages. When the erosion surface level was higher, upward migrations may have occurred from the reactor zone up into the overlying reducing black shales (fig. 9). This occurred between 350 Ka and 1.5 Ma ago. Then, erosion, accompanied with a downwardly penetrating redox/weathering front, continued until recently (<350 Ka) when the redox front began to penetrate into the reducing black shales. The estimated rate of downward redox front movement is 1.5 m / 100 000 years which also corresponds to the erosion rate if we assume that erosion plays a dominant role over the rate of movement of the redox front. This value is rather similar to those determined at Poços de Caldas where the rate of front movements varies between 2 and 20 m My⁻¹ for two fronts where oxidized rocks overlies reduced rocks (McKenzie et al., 1992).

Finally, disequilibria observed between ^{226}Ra and short-lived ^{214}Pb , ^{214}Bi and ^{210}Pb reveal that the Bangombé system has remained hydrodynamically active during the last century. A striking feature is the recent (<100 years) loss and leaching of Pb from the reactor core and the high-grade uranium ore, and its subsequent accumulation in surrounding shales.

ACKNOWLEDGEMENTS

This work was financially supported by the Swedish Nuclear Fuel & Waste Management Company (SKB), the French Agence Nationale de la Gestion des Déchets Radioactifs (ANDRA) and the Japan Atomic Energy Research Institute (JAERI). The cooperation of the Commissariat à l'Énergie Atomique, Direction du Cycle du Combustible (CEA/DCC) is gratefully acknowledged. R. Bros wishes to thank the Japan Science and Technology Agency (STA) for a fellowship.

REFERENCES

- Bros R., Stille P., Gauthier-Lafaye F., Weber F. and Clauer N. (1992) - Sm-Nd isotopic dating of Proterozoic clay material. Example from Francevillian sedimentary series (Gabon). *Earth Planet. Sci. Letters*, 113, p. 207-218.
- Bros R., Gauthier-Lafaye F., Larqué P., Samuel J., Stille P. (1995) - Mobility of U, Th, and Lanthanides around the Bangombé natural reactor (Gabon). *Mat. Res. Soc., Symp. Proc.*, 353, p. 1187-1195.

Bros R. and Gauthier-Lafaye F.(1996) - New drilling campaign and geological investigations on the Bangombé natural fossil reactor (Gabon) - Report of a field mission (September-December 1996). SKB Tech. Report, 31 p.

Bruno J., De Pablo J., Duro L., and Figuerola E. (1995) - Experimental study and modeling of the U (VI)-Fe(OH)₃ surface precipitation/coprecipitation equilibria. *Geochim. Cosmochim. Acta*, 59, p. 4113-4123.

Cancarz A.J. (1978) - U-Pb age ($2.05 \cdot 10^9$ years) of the Oklo uranium deposit. In: *Les réacteurs de fission naturels*, IAEA Vienne, p. 513-520.

Gascoyne M. (1989) - High levels of uranium and radium in groundwaters at Canada's Underground Research Laboratory, Lac du Bonnet, Manitoba. *Appl. Geochem.*, 4, p. 577-592.

Gauthier-Lafaye F. (1986) - Les gisements d'uranium du Gabon et les réacteurs d'Oklo. Modèle métallogénique de gîtes à fortes teneurs du protérozoïque inférieur. *Sci. Géol. Mém.*, Strasbourg, 206 p.

Griffault L.Y., Gascoyne M., Kamineni C., Kerrich R., and Vandergraaf T.T. (1993) - Actinide and rare earth element characteristics of deep fracture zones in the Lac du Bonnet granitic batholith, Manitoba, Canada, *Geochim. Cosmochim. Acta*, 57, p. 1181-1202.

Gurban I. (1996) - Caractérisation et modélisation de l'écoulement et du transport de matière au voisinage des réacteurs nucléaires naturels d'Oklo, Gabon. *Mém. Sci. Terre*, EM Paris, N°25, 194 p.

Hagemann R., Naudet R. et Weber F. (1980) - Enseignements tirés de l'étude des réacteurs naturels fossiles d'Oklo pour le stockage des déchets radioactifs. IAEA-SM-243/8, Vienne, p. 223-238.

Holliger P. (1992) - Les nouvelles zones de réaction d'Oklo : datation U-Pb et caractérisation *in-situ* des produits de fission à l'analyseur ionique. Note tech. DEM 01/92, CEREM Grenoble, 42 p.

Kaufman A. (1969) - Thorium-232 concentration of surface ocean water. *Geochim. Cosmochim. Acta*, 33, p. 717-724.

Louvat D., Toulhoat P. et Smellie J. (1995) - Caractérisation et modélisation des migrations à distance des zones de réaction. Synthèse des investigations hydrochimiques réalisées sur les sites d'Okélobondo et Bangombé. Rapport CEA/DCC/DESD, 58 p.

McKenzie A.B., Scott R.D., Linsalata P., and Mickleley N. (1992) - Natural decay series studies of the redox front system in the Poços de Calda uranium mineralisation. *Journal Geochem. Exploration*, 45, p. 289-322.

Morgan M.F. (1935) - The Universal Soil testing System. Connecticut Agricultural Experiment Station Bulletin 372.

Naudet R. (1991) - Des réacteurs nucléaires fossiles. Eyrolles, Paris, 695 p.

Osmond J.K., Cowart J.B., and Ivanovitch M. (1983) - Uranium isotopic disequilibrium in groundwater as an indicator of anomalies. *Inter. J. Appl. Rad. Isot.*, 34, p. 283-308.

Payne T. (1985) : Extraction and desorption of accessible uranium, in: *Radionuclide Migration around Uranium Ore Bodies - Analogue of Radioactive Waste Repositories*, AAEC Annual report, 1984 - 85, AAEC/C55, NUREG/CR-5040, p. 161-178.

Ruffenach J.C. (1979) - Les réacteurs nucléaires naturels d'Oklo. Paramètres neutroniques, date et durée de fonctionnement, migrations de l'uranium et des produits de fission. Thèse Sci., Univ. Paris VII, 351 p.

Salah S. and Gauthier-Lafaye F. (1997) - Preliminary study of Bangombé bore-holes : mineralogical and chemical data. Proceedings E.U. meetings, p. 47-80.

Smellie J. and Winberg A. (1991) - Background and status of SKB participation in the Oklo project (August 1990-August 1991), and future recommendations.

Smellie J. and Winberg A. (1993) - Preliminary reporting of CEA/EMP/SKB activities at Bangombé performed during September-December 1992.

Thiel K.R., Vorwerk R., Saager R., and Stupp H.D. (1983) - Uranium fission tracks and ^{238}U -series disequilibria as a means to study recent mobilization of uranium in Archean pyritic conglomerates. *Earth Planet. Sci. Lett.*, 65, p. 249-262.

Toulhat P., Gallien J.P., Louvat D., Moulin V., L'Henoret P., Guerin R., Ledoux E., Gurban I., Smellie J., Winberg A. (1994) - Preliminary studies of groundwater flow and migration of uranium isotopes around the Oklo natural reactors. Fourth Int. Conf. on the Chemistry and Migration behaviour of Actinides and Fission products, Charleston, USA, p. 383-390.

Yanase N., Nightingale T., Payne T. and Duerden P. (1991) - Uranium distribution in mineral phases of rock by sequential extraction procedure. *Radiochim. Acta*, 52/53, p. 387-393.

Yanase N. and Sekine K. (1995) - Measurement of uranium-series radionuclides in rock and groundwater at the Koongarra ore deposit, Australia, by gamma spectrometry. *Mat. Res. Soc. Symp. Proc.* Vol. 353, p. 1235-1242.

Zhang Ying-Jie, Bryan N.D., Livens F.R., Jones M.N. (1996) - Complexing of metal ions by humic substances. In *Humic and Fulvic Acids : Isolation, Structure and Environmental role*. Am. Chem. Soc., p. 194-206.